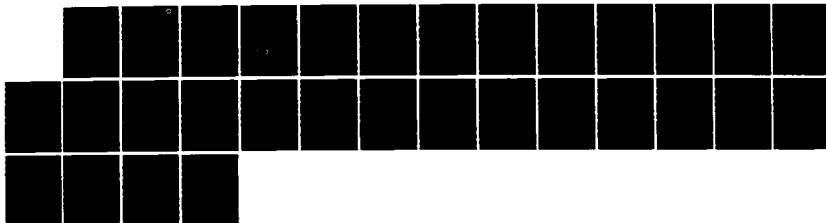AD-A173 449   HIGH EFFICIENCY TARGETS FOR HIGH GAIN INERTIAL   1/1
              CONFINEMENT FUSION(U) NAVAL RESEARCH LAB WASHINGTON DC
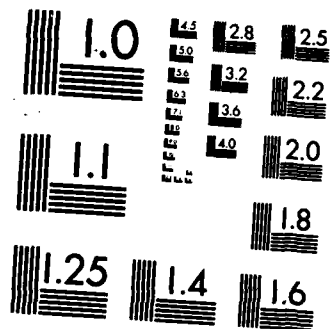   J H GARDNER ET AL. 19 SEP 86 NRL-MR-5814
UNCLASSIFIED   F/G 18/1   NL

MICROCOPY RESOLUTION TEST CHART

NATIONAL BUREAU OF STANDARDS-1963-A

AD-A173 449

High Efficiency Targets for High Gain Inertial Confinement Fusion

JOHN H. GARDNER AND STEPHEN E. BODNER

Laboratory for Computational Physics

DTIC FILE COPY

DTIC
ELECTE
OCT 2 4 1986

B

AD-A173 449

REPORT DOCUMENTATION PAGE

1a. REPORT SECURITY CLASSIFICATION UNCLASSIFIED			1b RESTRICTIVE MARKINGS			
2a. SECURITY CLASSIFICATION AUTHORITY			3 DISTRIBUTION/AVAILABILITY OF REPORT			
2b DECLASSIFICATION/DOWNGRADING SCHEDULE			Approved for public release; distribution unlimited.			
4. PERFORMING ORGANIZATION REPORT NUMBER(S) NRL Memorandum Report 5814			5 MONITORING ORGANIZATION REPORT NUMBER(S)			
6a. NAME OF PERFORMING ORGANIZATION Naval Research Laboratory		6b. OFFICE SYMBOL (If applicable) 4040	7a NAME OF MONITORING ORGANIZATION Department of Energy			
6c. ADDRESS (City, State, and ZIP Code) Washington, DC 20375-5000			7b. ADDRESS (City, State, and ZIP Code) Washington, DC			
8a. NAME OF FUNDING/SPONSORING ORGANIZATION Department of Energy		8b. OFFICE SYMBOL - (If applicable)	9. PROCUREMENT INSTRUMENT IDENTIFICATION NUMBER			
8c. ADDRESS (City, State, and ZIP Code) Washington, DC 20545			10. SOURCE OF FUNDING NUMBERS			

10. SOURCE OF FUNDING NUMBERS			
PROGRAM ELEMENT NO. DOE	PROJECT NO. DOE	TASK NO 81425	WORK UNIT ACCESSION NO.

11. TITLE (Include Security Classification)

High Efficiency Targets for High Gain Inertial Confinement Fusion

12. PERSONAL AUTHOR(S)
Gardner, John H. and Bodner, Stephen E.

13a. TYPE OF REPORT Interim	13b TIME COVERED FROM _____ TO _____	14 DATE OF REPORT (Year, Month, Day) 1986 September 19	15 PAGE COUNT 30

16. SUPPLEMENTARY NOTATION

17	COSATI CODES		18. SUBJECT TERMS (Continue on reverse if necessary and identify by block number)
FIELD	GROUP	SUB-GROUP	Efficiency
			Inertial Confinement Fusion
			Hydrodynamics

19 ABSTRACT (Continue on reverse if necessary and identify by block number)

Rocket efficiencies as high as 15% are possible using short wavelength lasers and moderately high aspect ratio pellet designs. These designs are made possible by two recent breakthroughs in physics constraints. First is the development of the Induced Spatial Incoherence (ISI) technique which allows uniform illumination of the pellet and relaxes the constraint of thermal smoothing, permitting the use of short wavelength laser light. Second is the discovery that the Rayleigh-Taylor growth rate is considerably reduced at the short laser wavelengths. By taking advantage of the reduced constraints imposed by nonuniform laser illumination and Rayleigh-Taylor instability, pellets using 1/4 micron laser light and initial aspect ratios of about 10 (with in flight aspect ratios of about 150-200) may produce energy gains as high as 200-250.

20 DISTRIBUTION/AVAILABILITY OF ABSTRACT ☒ UNCLASSIFIED/UNLIMITED ☐ SAME AS RPT ☐ DTIC USERS	21 ABSTRACT SECURITY CLASSIFICATION UNCLASSIFIED	
22a NAME OF RESPONSIBLE INDIVIDUAL John H. Gardner	22b TELEPHONE (Include Area Code) (202) 767-3055	22c OFFICE SYMBOL Code 4040

DD FORM 1473, 84 MAR   83 APR edition may be used until exhausted   SECURITY CLASSIFICATION OF THIS PAGE
All other editions are obsolete

CONTENTS

DTIC
SELECTED
OCT 2 4 1986
B

Accession For

NTIS CRA&I	✓
DTIC TAB	☐
Unannounced	☐
Justification	

By.
Distribution/

Availability Codes

| | Avail and/or |
| Dist | Special |

A-1

HIGH EFFICIENCY TARGETS FOR HIGH GAIN INERTIAL CONFINEMENT FUSION

I. INTRODUCTION

In the design of an inertial fusion pellet, one of the key variables is the coupling efficiency η, which is defined as the ratio of the kinetic energy in the imploding pellet divided by the incident driver energy. Figure 1 shows a typical plot of pellet gain versus laser energy for different coupling efficiencies, using the analytic isobaric model of Meyer-ter-Vehn. [1] For a reactor scenario in which one has to achieve some fixed minimum pellet gain, these curves show that the laser energy requirement increases somewhat faster than $1/\eta$. Alternatively, if one is limited to some maximum affordable laser, then the pellet gain increases faster than η. In this paper we will describe a new regime for direct-drive laser fusion that produces surprisingly high efficiency, while still consistent with the other physics constraints such as symmetry, preheat, and hydrodynamic stability.

For direct-drive laser fusion the overall coupling efficiency can be defined as the product of two parameters: the absorption efficiency and the hydrodynamic (or rocket) efficiency. With short wavelength lasers the time-integrated absorption efficiency can be about 70%. In our computational study, to be discussed below, we have found a regime with hydrodynamic efficiency of about 15%. The product of these two then gives an overall efficiency of about 10%. With an efficiency of about 10% Fig. 1 suggests that one can achieve very attractive pellet gains, of order 200-250, or more.

Rocket efficiency is controlled by a number of factors which we will discuss later in this article. Here we would like to mention two of them: the plasma blowoff velocity and sphericity. A rocket is most efficient when the blowoff velocity is appoximately equal to the rocket velocity; in laser fusion the plasma blowoff velocity is several times higher than the rocket implosion velocity. To minimize this high blowoff velocity one wants to use either a low laser intensity (and thus a thin pellet shell) or a short laser wavelength, or both. Sphericity effects will also reduce the rocket efficiency if the laser energy is absorbed on a

surface that is much larger in area than the ablation surface. To minimize this spherical effect, one wants to use either short laser wavelengths that absorb at high densities nearer the ablation front, or use large thin pellets with a high aspect ratio, $R/\Delta R$, such that the absorption and ablation surfaces are nearly equal in area. Spherical effects can also be minimized by accelerating the pellet before it converges significantly. Thus one wants to avoid excessive "pulse shaping".

The first pellet concept with really high coupling efficiency was proposed by Afanase'ev et. al. in 1975[2]. Their design achieved a hydrodynamic efficiency of 15% by using very large and very thin shells with an initial aspect ratio as high as 100, and by using moderate pulse shaping to limit the maximum laser intensity to about $10^{13}W/cm^2$ with one micron laser light. At this low an intensity the plasma blowoff velocity was low, the absorption high, and there was little risk of fast electron preheat.

This pellet design has been criticized because it uses such thin pellet shells. In particular, both experiments and simulations[3] at our laboratory indicate that these thin shells with one-micron light would be Rayleigh-Taylor unstable with a growth rate of about one-half the classical value of $\sqrt{kg}$. With this growth rate, the pellet shells would almost certainly break up before imploding. (Near-term experiments with very thin shells can sometimes produce preheat from thermal x-rays and thereby mask the hydrodynamic instability.)

The alternative approach to pellet design has been to be much more conservative on the pellet aspect ratio, with initial aspect ratios in the range of 5:1 to 3:1[4]. These thicker targets require much higher laser intensities to drive them. In this approach to avoid plasma instabilities which scale as $I\lambda^2$, the laser wavelength is reduced to either 1/3 or 1/4 micron. However, because the pellet shells are so thick, the laser intensity is still high enough that the design is above threshold for various plasma instabilities. Also with these

high intensities the rocket efficiency is low, in the range of 8% to 2%. This then implies relatively low pellet gains and high ignition energies.

In addition, there is very little thermal smoothing of laser nonuniformities when one uses either low intensity one-micron light or high intensity quarter-micron light. Laser nonuniformities are then directly impressed on the pellet, driving strong asymmetries and large amplitude Rayleigh-Taylor waves. Thus both approaches to laser fusion (very thin shells with $1\mu m$ laser light, and very thick shells with $1/3$-$1/4\mu m$ laser light) seem unsatisfactory.

Two breakthroughs in the last few years have radically changed the design constraints on direct-drive laser fusion, and are the motivating factors in this study of efficiency. First, a new optical technique called Induced Spatial Incoherence (ISI)[5] can dramatically improve the quality of a laser beam so that it can, without significant thermal smoothing, produce sufficiently uniform illumination to implode a pellet. The amount of thermal smoothing varies approximately[6] as $I\lambda^{2.7}$ (for $.5 \leq \lambda \leq 3\mu m$); the reduced reliance on thermal smoothing means that we can use much shorter laser wavelengths. Second, 2D computer simulations show that with these shorter laser wavelengths the growth rate for the Rayleigh-Taylor instability is only 30% of the classical value[7]. With the lower growth rate we can use thinner pellet shells.

In this paper we will examine the impact of using quarter-micron laser light with pellets whose initial aspect ratio is about 10:1. To minimize the spherical effects, we chose a pulse shape such that the pellet reaches its final kinetic energy when driven half-way inward at constant power, (and nearly constant acceleration). We assume without proof that this type of pulse shape can produce the correct entropy profile such that the pellet will successfully ignite and burn.

To provide an estimate of the effects of the Rayleigh-Taylor instability we assume that

3

the growth rate will be some constant fraction ϵ of the classical Rayleigh-Taylor growth rate. For spherical coordinates the planar classical growth rate $\sqrt{kg}$ goes over to $\sqrt{lg/R}$. Thus the total number of e-foldings is given by the expression

$$\gamma t = \epsilon \int^t dt' \sqrt{gl/(R_0 - gt'^2/2)}.$$

For nearly constant acceleration to $R_0/2$ this gives $\gamma t = \epsilon\sqrt{2l}\pi/4$. Our 2D nonlinear simulations show that the most dangerous perturbation wavelength is about three times the shell thickness[8]. Therefore we take $\lambda = 2\pi R_0/l \approx \pi\Delta R$ or $l \approx 2R_0/\Delta R$ giving the total growth in terms of the aspect ratio $R_0/\Delta R$ as $\gamma t = 0.5\epsilon\pi\sqrt{R_0/\Delta R}$. To find the amplitude of the Rayleigh-Taylor perturbation we need some estimate of the initial perturbation amplitude. To find the initial perturbation amplitude, let us assume that we have a high-gain pellet with initial radius R_0 of 3-4 millimeters and initial thickness ΔR_0 of 300-400 microns. During the initial phase of acceleration the shell is isentropically compressed about 20-fold to a thickness of about 15-20 microns. Assuming that the pellet can be manufactured with a surface finish of 1000Å for a perturbation wavelength of order 50 microns, this perturbation will be compressed to about 50Å. If we now assume that the perturbations at the end of the acceleration must be no more than 1/4 of the shell thickness, to allow for additional growth during the deceleration phase, then the allowable in-flight aspect ratios can be related to the initial perturbation A_0 by the relation

$$0.25\Delta R = A_0 e^{0.5\epsilon\pi\sqrt{R/\Delta R}}.$$

In table I we show the allowable aspect ratios as a function of the reduction in the classical growth rate. With a growth rate of 0.3 times the classical value, moderately thin pellet shells can be successfully imploded with initial aspect ratios of about 10 and in-flight aspect ratios of up to 200.

The ideas that shorter laser wavelengths, thinner shells, weak pulse shaping, and larger pellets lead to higher rocket efficiency is of course not new. What we have done for

the first time is to combine all of these ideas and optimize them. With these conditions we have a new regime with a new, very high rocket efficiency, approximately 15%. As we discussed above, one other study has found a similar efficiency, but they used an initial aspect ratio of 100 and a laser wavelength of 1 micron, as compared to our initial aspect ratio of 10 and 1/4 micron laser wavelength. Other studies with short laser wavelength have found much lower rocket efficiencies, of order 2-8%[9,10].

The results in this article were developed using a spherical 1-D Eulerian, sliding zone, FCT computer code.[11] It would obviously be attractive to also have an analytic formulation of the scaling laws for rocket efficiency. We have not succeeded because the regime with the highest rocket efficiency is also the least tractable for any analytic formulation. The problem is illustrated in Fig. 2. The number density, temperature, and laser intensity all continuously vary from the critical surface down into the the underdense plasma, with the absorption region overlapping the Mach 1 location. There is no natural boundary or boundary condition between the dense shell, the conduction region, and the absorption region; and no isothermal or adiabatic plasma approximation can be used to connect the outer plasma with the conduction region. The model of Max, McKee, and Mead[12] is also inapplicable because it requires a free-streaming region above the critical density region, and there is no such region with short-wavelength lasers at moderate laser intensities. Thus the complete set of equations must be integrated including a continuous absorption region. Nicolas and Sanmartin have recently reported a more complete model that reduces the problem to that of a quadrature and solves the problem in the limit of large charge number Z_i to avoid ion temperature effects[13]. They obtain analytic results for the deflagration regime but not for the complete range needed for this study (their parameter $\hat{W}$ which must be less than one for the deflagration regime exceeds 50 for our parameters). We have therefore chosen the more direct approach of direct numerical intergration of the partial differential equations. In the next section we describe the numerical model we used to

5

solve the equations.

II. MODEL

The calculations of hydrodynamic efficiency were performed using a one-dimensional spherical hydrodynamics code with the Flux-Corrected Transport numerical technique and an adaptive gridding scheme. A number of features make this code somewhat different from the usual codes that have been used to perform hydrodynamic simulations of laser-plasma interactions. Rather than being Lagrangian, the code uses an adaptive gridding technique to determine the location of zones in the calculation. This permits a redistribution of the zones to regions that require the greatest resolution. This is primarily in the ablation region and in the region of maximum laser absorption. The primary zone size is controlled by the mass per zone much as in a Lagrangian code, however the mass per zone is not required to remain fixed as in a Lagrangian code. Rather material is allowed to flux through zone boundaries in a controlled manner.

To achieve this control the imploding shell is divided into three regions 1) the cold dense compresssed region, 2) the ablation region out to the critical surface, and 3) the region beyond the critical surface. The cold dense shell is treated in a manner very similar to Lagrangian codes with the zones moving nearly at the fluid velocity and the mass per zone kept nearly constant until compression to several times solid density. Compression beyond that point does not produce a further decrease in zone size but rather the zone size becomes fixed and material flows through the zone boundaries. In the ablation region the mass per zone is made proportional to the density; thus the zone size remains nearly constant, maintaining high resolution of the ablation surface. When the mass per zone decreases below a critical value determined by the resolution required at the critical surface, the mass per zone is held fixed. Beyond the critical surface the mass per zone is allowed to slowly increase so as not to waste zones in the very underdense region where very

6

little absorption takes place. In addition to this primary zone control, a further adaptive gridding procedure is employed to cluster zones in regions of high gradient: the mass per zone is decreased by a term inversely proportional to the gradient of the density. The zone adjustment is performed in a routine that computes the ideal zone mass distribution and then diffuses the zone locations at each step to move toward that ideal distribution.

This kind of zone motion is permitted by the use of the sliding-zone Flux-Corrected Transport (FCT)[14] which solves continuity-type equations for the fluxes relative to moving zone boundaries. One distinctive feature of this numerical algorithm is that no artificial viscosity is expicitly required to maintain numerical stability, while the overall scheme is second-order accurate. Thus mass, momentum and energy are locally and globally conserved. This is in contrast to many of the codes currently in use where the mass and momentum are conserved but a nonconservative form of the energy equation is used. An artificial viscosity is required in those codes to account for any shock heating. While many clever choices of this artificial viscosity can conserve energy in a number of idealized problems there is no way to guarantee this in general. In laser ablation problems, claims have been made for a high degree of energy conservation using codes of this type. However, a large fraction of the energy is tied up in the expanding hot plasma where no shocks are expected, and where the artificial viscosity plays no role. The cold dense part of the target, however, has only a small fraction of the energy and most of that is kinetic. Thus a relatively large error could be made in the internal energy (pressure) with only a small error showing up in the total energy. Futhermore, errors in one region may be compensated for by additional errors in another region. Only local conservation can avoid this difficulty. We emphasize the numerical aspects of the solution since the results for the solution of any physical model equations are no better than the accuracy of the methods used to solve them.

A study by Pollaine and Lindl has come to a more pessimistic conclusion about the

7

possibilities of high gain[9]. We note here however that their model uses a treadmill rezoner in the blowoff region which cannot simultaneously conserve mass, momentum, and energy. Their claim is that this rezoning is beyond the Mach 1 position so that it does not effect the hydrodynamic efficiency. However, due to thermal conduction the sonic point does not decouple the outer solution from the ablation region. Futhermore, the solution in the outer region can effect the inverse bremsstrahlung absorption thoughout the solution region which determines where the laser energy is absorbed, and then can affect the hydrodynamic efficiency. Whether this accounts for the somewhat lower hydrodynamic efficiencies found in their study is as yet an open question.

The physical model used here is based on a collisional fluid model. A one-temperature model is used for most of the calculations although the effects of this compared to a two temperature model will be discussed later. The equations for the conservation of mass, momentum and energy are solved using the conservative finite difference scheme discussed above. Thermal conduction is treated by the model of Spitzer and Harm[15] with the additional constraint that the thermal flux is limited by a fraction of the free-streaming velocity of the electrons. This is accomplished by taking the harmonic mean of the Spitzer conduction and the free-stream limit. The fractional value of 0.1 suggested by the results of Fokker-Planck codes is used[16]. No additional flux limiting beyond this is assumed. For the plasma scalelengths associated with reactor scale targets, the flux limiting plays almost no role.

The fluid equations are closed with equations of state that express $P = F(e, \rho)$ and $T = G(e, \rho)$. To model the cold fuel region these must include the effect of high density solid material, Fermi-temperature and fractional ionization. We based our equation of state on the solid material models used in the analytic model (ANEOS) in the CHARTD code[17], and expansions of the Fermi-Dirac functions by Clayton[18]. This includes the effect of a Debye-Grüneisen model near solid density and goes smoothly from a Thomas-Fermi-Dirac

model for degenerate electrons at high density and low temperature to a Saha equilibrium model at high temperatures and low densities.

The laser beam is assumed to be made up of an infinite number of beams, each in the far-field of a high focal number lens, with a focal distribution given by an ISI produced laser beam. This allows the use of uniform illumination needed for a one dimensional code while allowing for the effects of a finite ray geometry. A finite number of rays are traced through the plasma corona to model the effect of ray curvature on the absorption process. The laser absorption in this code is classical inverse bremsstrahlung absorption.

The targets used in this study are made up entirely of initially frozen DT. The choice of DT as a ablator as well as for the final fuel is motivated by the desire to minimize the effects of radiation preheat by using as low a Z ablator as possible. The hydrodynamics is only affected by the ratio of Z/A (the ratio of the atomic charge to the atomic number which is nearly equal to $1/2$ for all atomic species). Considerations of how to manufacture such a target is not considered here except to say that a thin layer of plastic could be used to form a initial seed layer on which to deposit the DT both on the inside and the outside. For the purposes of this study the radius of the DT shell is chosen so that after the ablation is complete, 1 mg of DT remains to form the imploding shell. Thus for an initial aspect ratio of 9 the initial shell radius would be about 2 mm (about $1/2$ of the initial DT is ablated away during the laser pulse). The target is initially started as a $210 \mu m$ thick shell at nearly zero temperature with an inner radius of $1986 \mu m$. The region inside the target is filled with DT vapor at a density of $1.25 \times 10^{-4} gm/cm^2$.

A moderate amount of pulse shaping was used. A low intensity foot was used to shock heat the DT to the proper isentrope followed by a gradually increasing laser pulse designed to provide nearly shock free further compression of the target. Following the suggestion of J. Lindl[19] the peak of the laser intensity is timed so that the final compression wave

arrives at the rear of the shell nearly coincident with shock breakout. Small errors in the timing of the peak intensity result in an increasing fraction of the inner edge of the target being placed on too high an isentrope. Final target entropy is controlled by the ratio of the initial to the final laser intensity, which also controls the time delay between the initial pulse and the peak of the pulse. The laser power is then held constant for sufficient time to accelerate the imploding shell to a velocity of $3.5 \times 10^7 cm/sec$ while the target has moved to 1/2 of its initial radius. This latter requirement also determines the magnitude of the peak of the laser pulse. The laser beam is then shut off and the target allowed to coast to its final implosion at the center.

During the initial compression phase the target does not move very far but the effective aspect ratio is greatly increased. The in-flight aspect ratio (IFAR), (defined as the inner radius of the target divided by the distance between the two radii of the target where the density drops to 1/e of the peak density), increases from its initial value of about 10 to values nearly 20 times that great. Because the target is compressed to this high aspect ratio before significant shell acceleration begins we express our results in terms of the compressed IFAR rather than the initial aspect ratio of the target. Also different materials used as an ablator will compress by different amounts. The relatively light DT will compress more that a heavier high Z material. Mass ablation rates are also insensitive to material. Thus it is the initial mass of the shell that is important rather than the initial aspect ratio.

Finally, for the purposes of this study the hydrodynamic efficiency will be defined as the ratio of the kinetic energy of all the material moving toward the center divided by the absorbed laser energy. (This involves only a small error since only a small fraction of the inward kinetic energy is contained in the region behind the dense shell where the density is low.) The total efficiency is defined as the inward kinetic energy divided by the total laser energy and thus includes an absorption efficiency.

10

III. RESULTS

In accordance with the rocket model, the hydrodynamic efficiency depends on the final velocity of the implosion. For this study we used a fixed value of $v_f = 3.5 \times 10^7 cm/sec$. This is a sufficiently high value to provide the necessary compression of the cold fuel and to provide a sufficiently high temperature in the central spark region for ignition. To study the effect of variation in laser wavelength on efficiency we hold the final mass and aspect ratio of the pellet fixed and adjust the laser intensity to produce the required ablation pressure necessary to drive the pellet to its required velocity at 1/2 of the pellet radius. The results are shown in Fig. 3. There is a significant advantage in the use of 1/4 micron light rather than 1/3 micron light. The hydrodynamic efficiency from the rocket model scales like $\eta \propto (v_f/v_e)^2/(\exp(v_f/v_e) - 1)$ where v_e is the exhaust velocity and the proportionality constant depends on details of the corona blowoff[20]; for small v_f/v_e this is proportional to v_f/v_e. Thus the rocket efficiency is inversely proportional to the blowoff velocity. The shorter laser wavelengths absorb the energy at higher density and lower temperature thus producing a lower blowoff velocity and a higher hydrodynamic efficiency. The shorter laser wavelength also increases the absorption efficiency and thus increases even further the total efficiency.

Since the hydrodynamic efficiency is closely related to the blowoff velocity, it is also dependent on the ablation pressure and laser intensity. From simple geometrical considerations one finds for our case of nearly uniform acceleration to one half of the shell radius that the final shell velocity is given by $v_f \propto \sqrt{(P/\rho)(R_0/\Delta R)}$ which means the ablation pressure is inversely proportional to the aspect ratio of the pellet. The maximum IFAR that can be imploded is determined by limits imposed by the Rayleigh-Taylor instability as discussed in the introduction. The increased ablation pressure and laser intensity required as the aspect ratio is decreased result in a decrease in the hydrodynamic efficiency. In Fig. 4 we show the effect of the IFAR on the hydrodynamic efficiency. A factor of

two increase in IFAR produces about a factor of two increase in efficiency. The IFAR in turn depends on two factors, the ablation pressure and the isentrope. The latter can be conveniently measured as the ratio of the fuel pressure to the pressure it would have if the temperature were zero. In our simulations the ratio of the pressure to the cold pressure was approximately 3 and was determined by the strength of the initial shock.

The effect of the aspect ratio is felt in a second way. A lower aspect ratio requires a higher ablation pressure to achieve the same final velocity; this in turn requires a higher laser intensity. The higher ablation pressure also compresses the target to a yet higher aspect ratio which requires a futher reduction in the initial aspect ratio to achive the same IFAR. Both ideal gas and fermi-degenerate equation's of state have $P \propto \rho^{5/3}$ or $\rho \propto P^{3/5}$. Where combined with the conservation of mass and a fixed implosion velocity this leads to a scaling of $R/\Delta R \propto P^{-2/5}$. From the intensity scaling $P \propto I^{7/9}$ for spherical implosions one obtains a very strong dependence of the intensity $(I \propto (R/\Delta R)^{-45/14})$ on the IFAR. Thus the IFAR not only affects the hydrodynamic efficiency but can lead to very high laser intensities at lower IFAR. For instance the shell with a IFAR of 200 and an initial aspect ratio of 13 had a peak irradiance near the end of the pulse of $2.2 \times 10^{14} W/cm^2$ while the shell with an IFAR of 100 and an initial aspect ratio of 5 required a peak intensity of $1.25 \times 10^{15} W/cm^2$ to accelerate the target to the same final velocity. See Fig (4b).

A number of calculations were performed to check the sensitivity of the results to various physical and numerical changes. As a check on the sensitivity to variations in the thermal conductivity, the $\ln \Lambda$ in the Spitzer conduction coefficient was varied in a number of ways. The lower limit on the value of $\ln \Lambda$ was varied between the values one to five. This primarily affected the conduction coefficient in the region near the ablation surface without changing it near the critical surface. The code was also run with constant values of $\ln \Lambda$ equal to three and 10; this should affect the conduction coefficient uniformily over the plasma. The results in Fig. 5 show little sensitivity of the hydrodynamic efficiency on

12

the conduction coefficient. In order to check the sensitivity to conductivity in the critical region, the flux limiter coefficient was varied from .03 to .5. This had the primary effect of reducing the heat flux to the ablation surface and heating the plasma corona to a higher temperature. As shown in Fig. 6, the rocket efficiency was little affected except at the lowest values of the flux limiter. The total efficiency droped considerably at these lower values of the flux limiter, primarily because of a reduced absorbtion efficiency by inverse bremsstrahlung. The use of strong flux limiting is currently less fashionable and values near 0.1 are most widely accepted, so that flux limiting should play almost no role in the calculation of hydrodynamic efficiency. Another sensitivity test was the size of the focal spot used to illuminate the pellet. In these calculations the focal disribution was assumed to be that of overlapped *double sinc* function (used in the ISI technique). A cylindrically averaged approximation to this profile is given by $I \propto \sin^4(\max(\tilde{x} - 0.5, 0))/(\max(\tilde{x} - 0.5, 0))^4$ where $\tilde{x} = 2\pi x/(\sqrt{2}d)$ and x and d are the distance from the center of the focal spot and the focal diameter respectively. As the focal spot diameter becomes nearly as large as the pellet, ray refraction causes a larger fraction of the laser light to either fail to be absorbed or to be absorbed in the low density corona where it cannot contribute effectively to the efficiency. In Fig. 7 we show both the total and the rocket efficiency as a function of the focal radius of the laser spot. Both the total and rocket efficiency drop off as the focal radius appoaches the $2mm$ pellet radius. (In a separate analysis, to be submitted for publication, A. Schmitt and J. Gardner show that the smaller focal spot suffices to produce adequate time-averaged uniformity on the pellet.) As mentioned earlier we also checked the sensitivity of our results to the use of a one-temperature model. For high Z materials the ions contribute only a small fraction to the internal energy and we would not expect a significant hydrodynamic difference between a one and two-temperature calculation. However for DT with a Z=1 the electron and ion internal energies are of the same order of magnitude and we expect some modification in the hydrodynamic calculation. There are basically two competing effects. The decoupling of the ion and electron temperatures

13

results in a higher electron temperature and higher blowoff velocity which decrease the hydrodynamic efficiency, however this is offset by the deeper penetration of the laser light and increased mass ablation rate which increase the hydrodynamic efficiency. The result is that the two-temperature model gives a slightly higher efficiency than that found in our one-temperature calculations; if anything, we are slightly pessimistic. As a final sensitivity check we have looked at the numerical resolution. Even in a fully conservative code the distribution of energy can depend on the resolution of the calculation. But using the flexibility in our code we can vary the resolution in various regions of the profile. We have found that the resolution seems to be most sensitive to the gridding at and beyond the critical surface, indicating that the results are most sensitive to the absorption processes, not the ablation region. This is consistent with the sensitivity to the conduction coefficient and the focal diameter. In Fig. 8 we plot the hydrodynamic efficiency as a function of the resolution at the critical surface, a measure of the underdense resolution. The minimum resolution shown is one micron. The corresponding resolution at the ablation surface is 600 Å.

As a final remark we note that a better match of the rocket velocity and the blowoff velocity would result in a higher efficiency, but then a rather large fraction of the target mass would be ablated away. This would exacerbate the effect of nonuniformities in the laser intensity. For wavelengths on the order of the pellet radius any asymmetry in the laser intensity results in a corresponding asymmetry in the pressure, ablated mass, and implosion velocity. If a large fraction of the target is ablated then the remainder of the target will suffer from an increased asymmetry due to the higher acceleration of the region of reduced mass. The optimum efficiency occurs for a mass ratio of $m_f/m_i = 0.2$. The mass ratio for the laser fusion case is about 0.5. However, because the target is much thinner near the end of the optimum efficiency case, the variation in acceleration is much greater, resulting in a much larger velocity nonuniformity. A more detailed calculation

14

of the effect shows that the optimum efficiency case will have a nonuniformity 2.5 times as great as that imposed by the typical laser driven implosion for the same illumination nonuniformity. Perhaps we should be happy that we cannot optimize blowoff velocity.

IV. CONCLUSIONS

These results indicate that if the Rayleigh-Taylor growth rate is reduced to 30% of its classical value at $1/4\mu m$ as predicted by detailed numerical simulations, so that pellets with an initial aspect ratio of ten and an IFAR on the order of 150-200 can be stably imploded, then hydrodynamic efficiencies as high as 15 percent are possible. This is a considerable improvement over the 2-8% that is possible if the IFAR aspect ratios are limited to less than 100. We note that the results for hydrodynamic efficiency appear to be insensitive to the details of the thermal transport, but the overall efficiency can be more sensitive to factors which affect the absorption region. Similar results with pellet masses of 1/2 milligram fuel mass suggest that these results are insensitive to pellet size if the pellet is sufficiently large.

The implications for reactor pellets are quite profound. While overall efficiencies of only a few percent would make high gain impossible, overall efficiencies of 10% provide the possibility for pellet gains greater than 200. The direction for pellet design is also then different. These results imply that the search for high gain pellets should be in the direction of short laser wavelength with a moderate aspect ratio (about 10) and moderate (not highly shaped) laser pulses of a few times 10^{15} W/cm^2 peak intensity. Two caveats are appropriate. This conclusion is based on the results of numerical simulations of the Rayleigh-Taylor instability that predict a sharply reduced growth rate with $1/4$ μm laser light. But to-date there is no experimental Rayleigh-Taylor data at this short laser wavelength. (Experiments using one micron laser wavelength show a reduction of growth below classical, and are consistent with simulations.)[21] In addition the high pellet gains

15

are predicted from rather simple models of the propagating burn. It has not yet been demonstrated that pellets using the moderate pulse shaping suggested here will actually produce a proper size, nearly spherical, propagating burn regime.

ACKNOWLEDGEMENTS

REFERENCES

1. J. Meyer-ter-Vehn, Nucl. Fusion, **22**, 561 (1982).

2. Yu.V. Afanas'ev, N.G. Basov, P.P. Volosevich, E.G. Gamalii, O.N. Krokhin, S.P. Kurdyu-mov, E.I. Levanov, V.B. Rozanov, A.A. Samarskii, and A.N. Tikhonov, ZhETF Pis. Red. **21**, 150 (1975) [JETP Lett. **21**, 68 (1975)].

3. M.H. Emery, J.H. Gardner, and J.P. Boris, Phys. Rev. Lett. **48**, 677 (1982).

4. C.P. Verdon, R.L. McCrory, P.W. McKenty, and S. Skupsky, Bull. Am. Phys. Soc. **30**, 1482 (1985)

5. R.H. Lehmberg and S.P. Obenschain, Optics Commun. **46**, 27 (1983); S.P. Obenschain, Bull. Am. Phys. Soc. **30**, 1382 (1985).

6. J.H. Gardner and S.E. Bodner, Phys. Rev. Lett. **47**, 1137 (1981).

7. M.H. Emery, Bull. Am. Phys. Soc. **29**, 1231 (1984).

8. M.H. Emery, J.H. Gardner, and J.P. Boris, Appl. Phys. Lett. **41**, 808 (1982).

9. S.M. Pollaine and J.D. Lindl, (*submitted to Nuclear Fusion*), (1985).

10. C.E. Max, J.D. LIndl, and W.C. Mead, Nucl. Fusion **23**, 131 (1983).

11. J.H. Gardner and S.E. Bodner, Phys. Rev. Lett. **47**, 1137 (1981).

12. C.E. Max, C.F. McKee, and W.C. Mead, Phys. Fluids **23**, 1620 (1980).

13. J.A. Nicolás and J.R. Sanmartin, Plasma Physics **27**, 279 (1985).

14. J.P. Boris and D.L. Book, Methods Comput. Phys. **16**, 85 (1976).

15. L. Spitzer Jr. and R. Harm, Phys. Rev. **89**, 977 (1953).

16. A.R. Bell, R.G. Evans, and D.J. Nicholas, Phys. Rev. Lett. **46**, 243 (1981).

17. S.L. Thompson and H.S. Lauson, (*private communication*).

18. D.D. Clayton, *Principles of Stellar Evolution and Nucleosynthesis* (McGraw-Hill, New York, 1968).

19. J.D. Lindl, (*private commuinication*).

20. J.R. Sanmartin, J.L. Montanés, J. Sanz, and R. Ramis, Plasma APhysics 27, 983 (1985).

21. J. Grun, M.H. Emery, S. Kacenjar, C.B. Opal, E.A. McLean, S.P. Obenschain, B.H. Ripin, and A. Schmitt, Phys. Rev. Lett. 53, 1352 (1984).

TABLE I

Allowable In-Flight-Aspect-Ratio (IFAR) as a Function
of the Reduction in Rayleigh-Taylor Growth Rate

	Classical	$1\mu m$ laser light	$1/4\mu m$ laser light
$\gamma/\sqrt{kg}$	1	0.5	0.3
IFAR	30	90	200

18
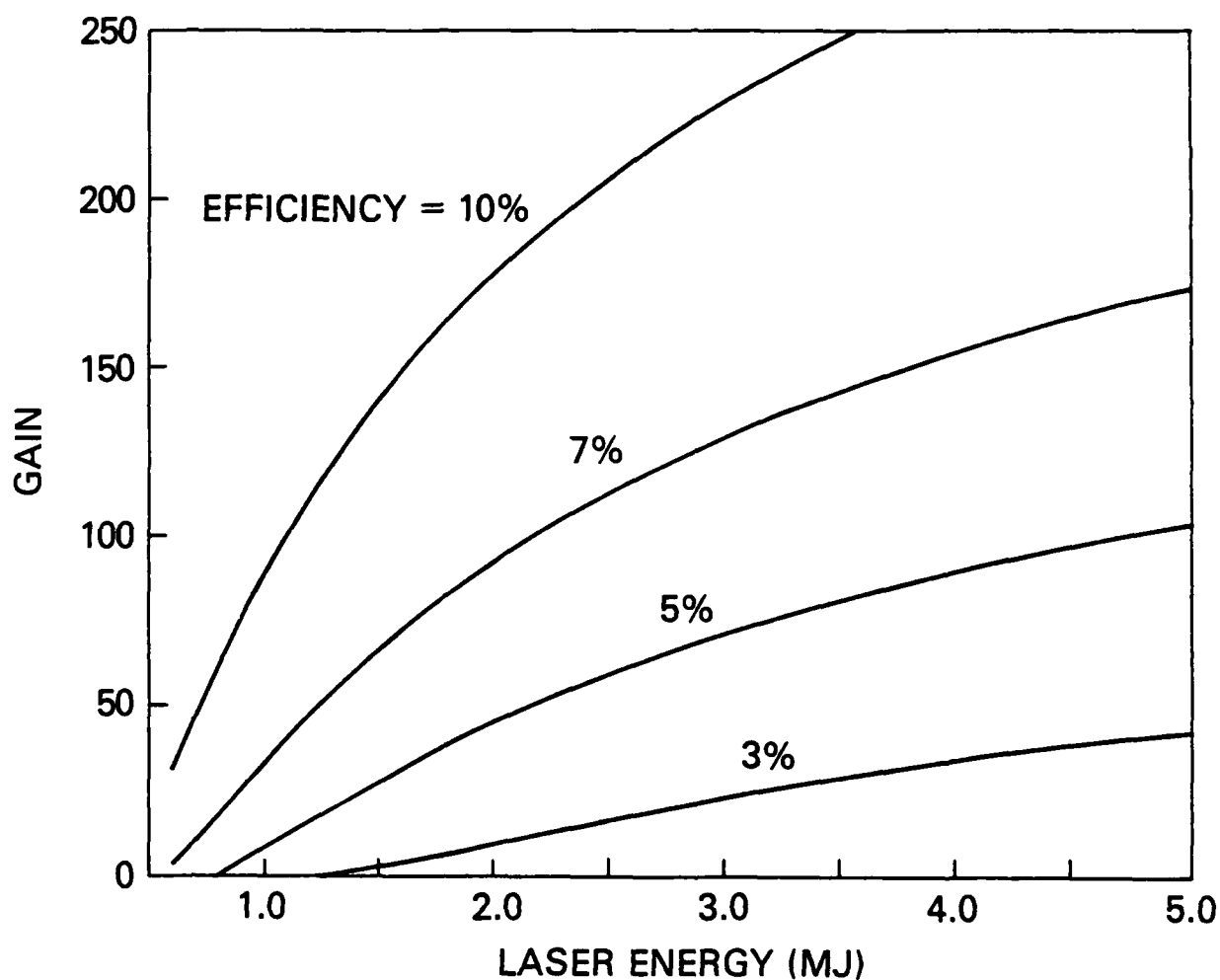
FIG. 1. Pellet gain as a function of the laser energy and coupling efficiency using the isobaric model of Meyer-ter-Vehn for hot spot ignition and propogating thermonuclear burn. The ignitor consisted of a 70 micron sphere of 50 g/cc DT at 5 KeV, with the cold fuel isentrope three times the Fermi-degenerate energy density.
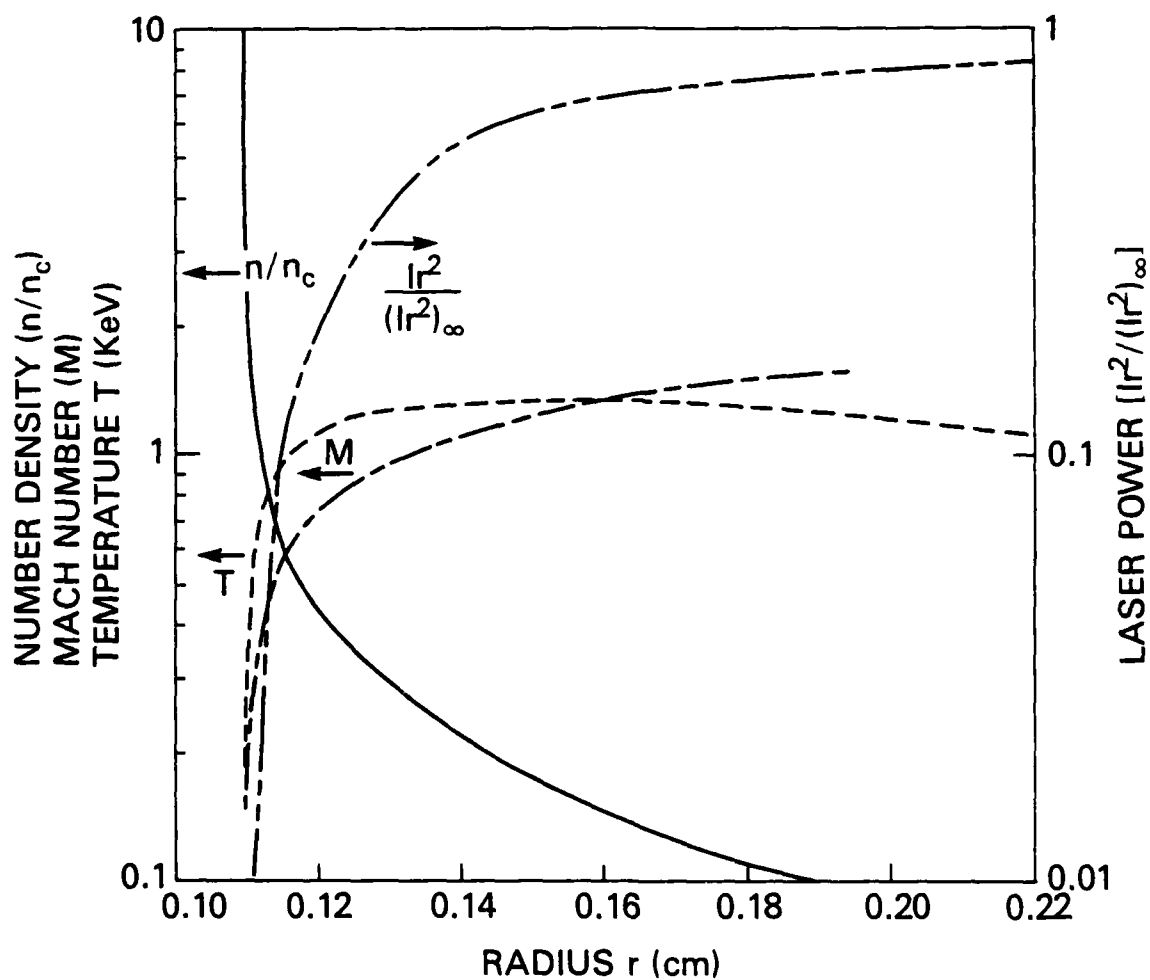
FIG. 2. Typical blowoff plasma variables as a function of radius from the ablation surface to the underdense corona.
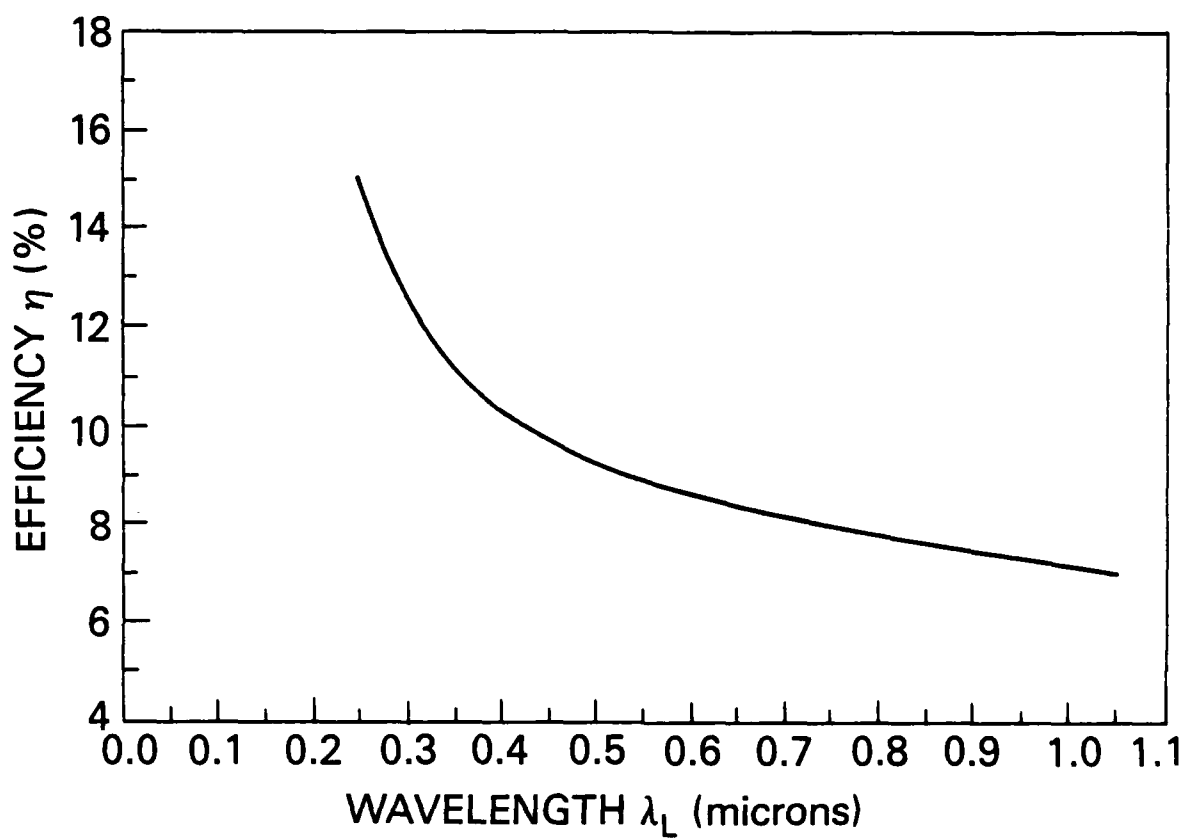
FIG. 3. Hydrodynamic efficiency as a function of the laser wavelength. Lower blowoff velocity and reduced spherical effects greatly increase hydrodynamic efficiency.
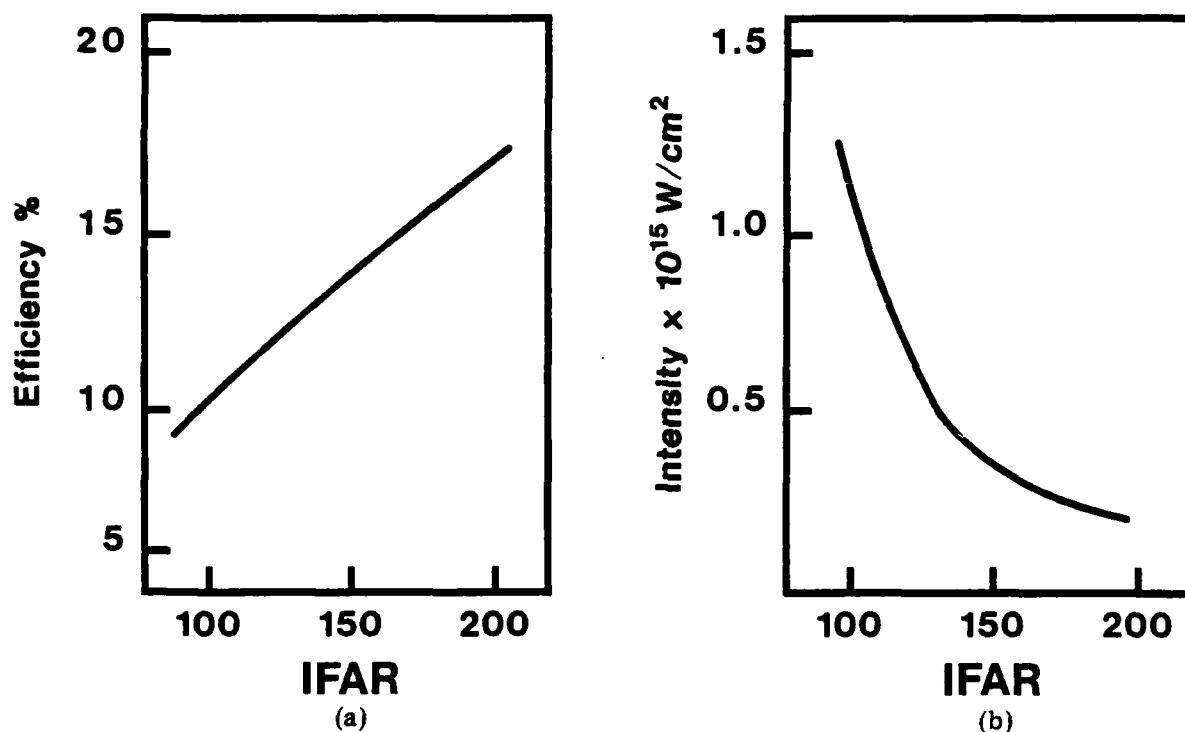
FIG. 4. Hydrodynamic efficiency (4a) and maximum laser intensity (4b) as a function of the in-flight aspect ratio (IFAR). The lower ablation pressure and laser intensity required to drive the thinner pellets results in a lower blowoff velocity, higher hydrodynamic efficiency and a reduced suceptibility to plasma instabilities.
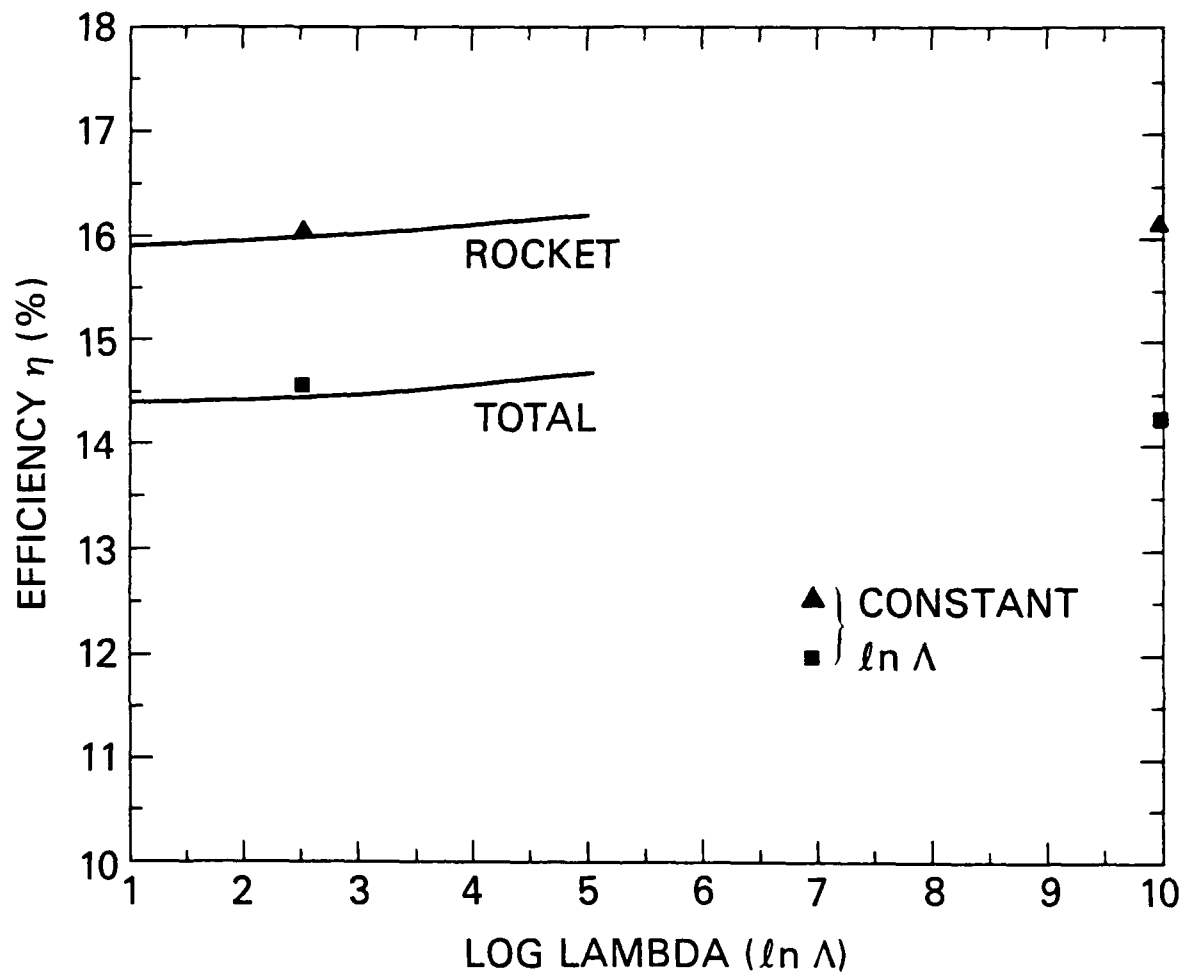
FIG. 5. The sensitivity of efficiency to details of thermal conduction in the overdense plasma was studied by varying the minimum $\ln \Lambda$ value in the Spitzer conductivity coefficient. A constant $\ln \Lambda$ of 3 and 10 was also used.
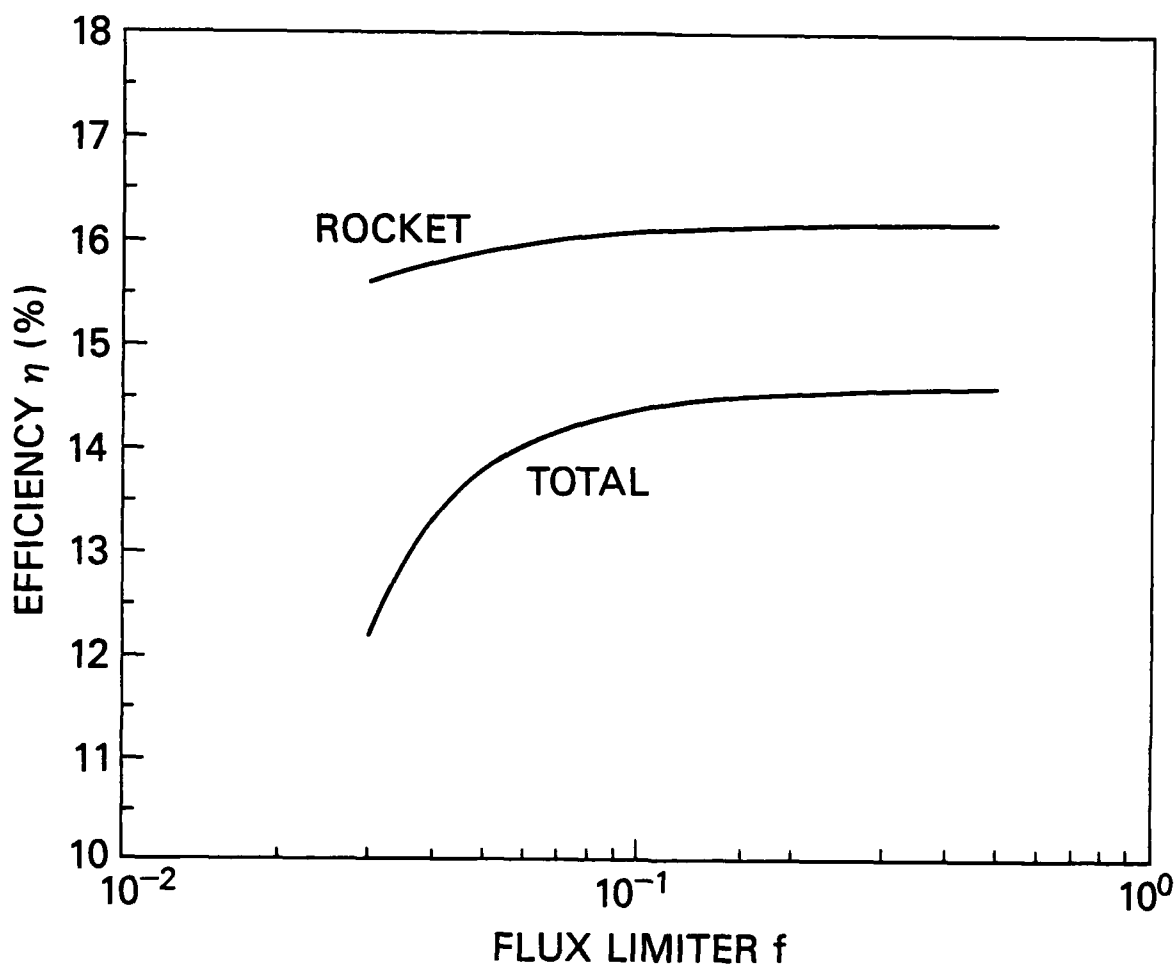
FIG. 6. The sensitvity of efficiency to thermal transport in the critical region was studied by varying the coefficient used in the flux limiter. The effect is large in overall efficiency (because of reduced inverse bremsstrahlung absorption) only in the strongly flux limited regime which is not applicable to the long scalelength plamas used for high gain targets.
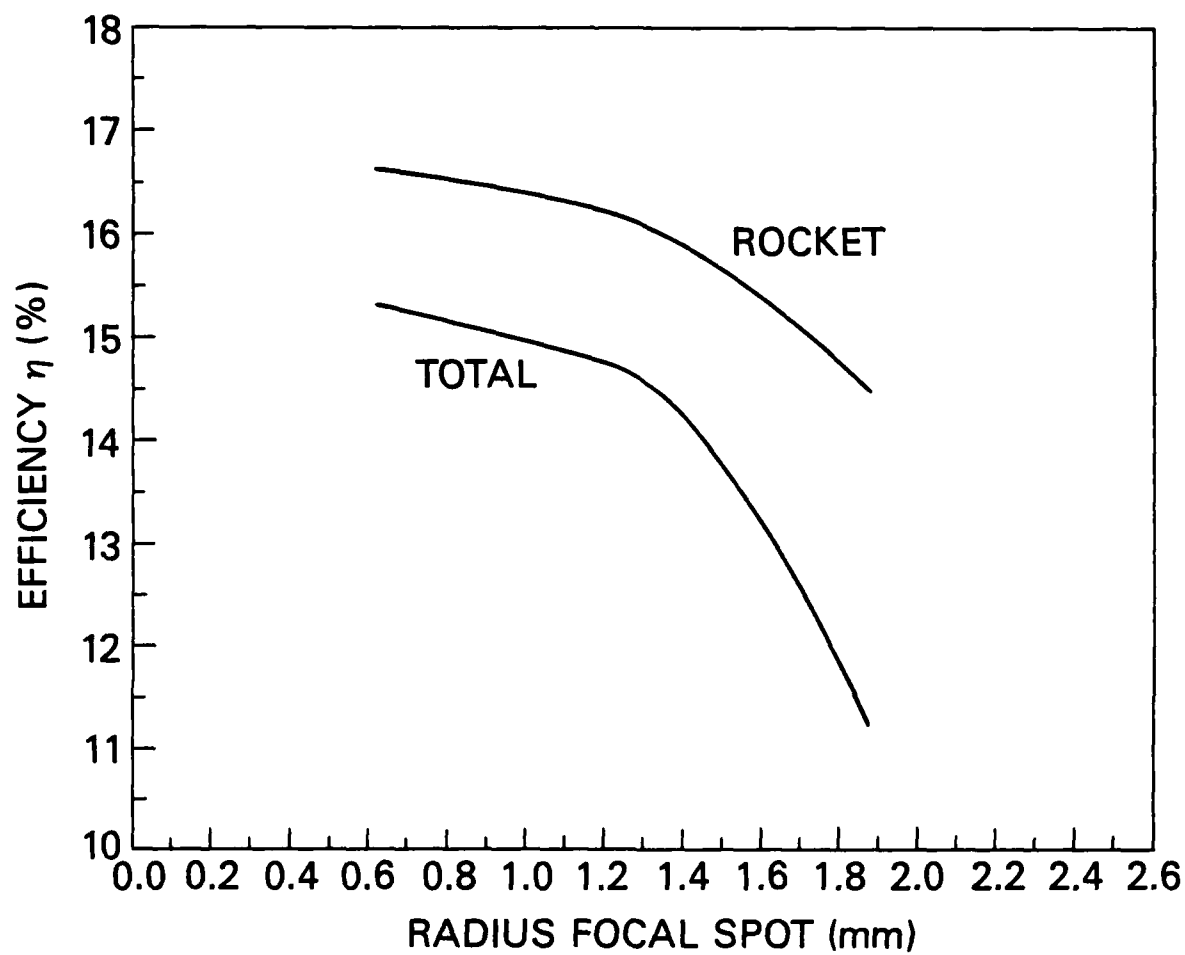
FIG. 7. The sensitivity of efficiency to the absorption details was studied by varying the focal diameter of the laser beam. As the beam radius becomes larger than the ablation radius, refraction reduces the absorption efficiency and causes absorption to take place at a larger radius reducing hydrodynamic efficiency.
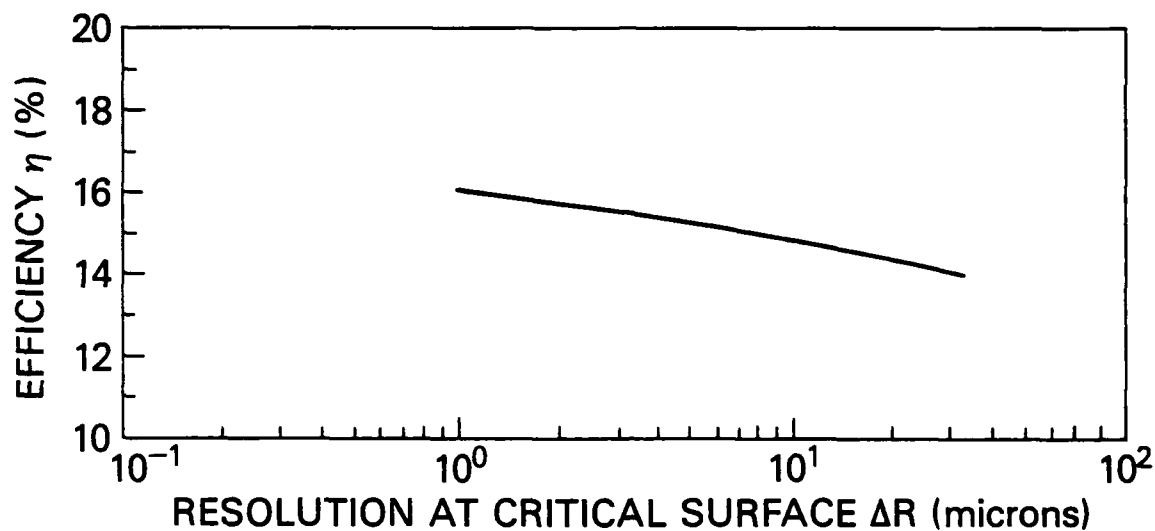
FIG. 8. The sensitivity of efficiency to numerical resolution was studied by varying the grid resolution. It was found that the efficiency was most sensitive to resolution in the underdense plasma where the inverse bremsstrahlung absorption was taking place.

END

12 - 86

DTIC